



## Identifying precursors and aqueous organic aerosol formation pathways during the SOAS campaign

Neha Sareen<sup>1</sup>, Annmarie G. Carlton<sup>1</sup>, Jason D. Surratt<sup>2</sup>, Avram Gold<sup>2</sup>, Ben Lee<sup>3</sup>, Felipe D. Lopez-Hilfiker<sup>3, a</sup>, Claudia Mohr<sup>3, b</sup>, Joel A. Thornton<sup>3</sup>, Zhenfa Zhang<sup>2</sup>, Yong B. Lim<sup>1, c</sup>, Barbara J. Turpin<sup>2\*</sup>

1. Department of Environmental Sciences, Rutgers University, 14 College Farm Road, New Brunswick, New Jersey 08901, United States

10 2. Department of Environmental Sciences and Engineering, Gillings School of Public Health, University of North Carolina at Chapel Hill, Chapel Hill, North Carolina 27599, United States

3. Department of Atmospheric Sciences, University of Washington, Seattle, Washington 98195 United States

<sup>a</sup>Now at Laboratory of Atmospheric Chemistry, Paul Scherrer Institute, 5232 Villigen PSI, Switzerland

15 <sup>b</sup>Now at Institute of Meteorology and Climate Research, Atmospheric Aerosol Research, Karlsruhe Institute of Technology, Karlsruhe, Germany

<sup>c</sup>Now at Center for Environment, Health and Welfare Research, Korea Institute of Science and Technology, Seoul 02792, Republic of Korea

\*bjturpin@email.unc.edu

20 *Correspondence to:* Neha Sareen (neha.sareen15@gmail.com)

**Abstract.** Aqueous multiphase chemistry in the atmosphere can lead to rapid transformation of organic compounds, forming highly oxidized low-volatility organic aerosol and, in some cases, light-absorbing (brown) carbon. Because liquid water is globally abundant, this chemistry could substantially impact climate, air quality, and 25 health. Gas-phase precursors released from biogenic and anthropogenic sources are oxidized and fragmented, forming water-soluble gases that can undergo reactions in the aqueous phase (in clouds, fogs, and wet aerosols) leading to the formation of secondary organic aerosol (SOA<sub>AQ</sub>). Recent studies have highlighted the role of certain precursors



like glyoxal, methylglyoxal, glycolaldehyde, acetic acid, acetone, and epoxides in the  
30 formation of SOA<sub>AQ</sub>. The goal of this work is to identify additional precursors and  
products that may be atmospherically important. In this study, ambient mixtures of water-  
soluble gases were scrubbed from the atmosphere into water at Brent, Alabama during  
the 2013 Southern Oxidant and Aerosol Study (SOAS). Hydroxyl (OH<sup>•</sup>) radical  
35 oxidation experiments were conducted with the aqueous mixtures collected from SOAS  
to better understand the formation of SOA through gas-phase followed by aqueous-phase  
chemistry. Total aqueous-phase organic carbon concentrations for these mixtures ranged  
from 92–179 μM-C, relevant for cloud and fog waters. Aqueous OH-reactive compounds  
were primarily observed as odd ions in the positive ion mode by electrospray ionization  
40 mass spectrometry (ESI-MS), indicative of alcohols, carbonyl compounds, and/or  
epoxides. Ultra high-resolution Fourier-transform ion cyclotron resonance mass  
spectrometry (FT-ICR-MS) spectra and tandem MS (MS/MS) fragmentation of these ions  
were consistent with the presence of carbonyls and tetrols. Products were observed in the  
negative ion mode and included pyruvate and oxalate, which were confirmed by ion  
45 chromatography. Pyruvate and oxalate have been found in the particle phase in many  
locations (e.g., as salts and complexes). Thus, formation of pyruvate/oxalate suggests the  
potential for aqueous processing of these ambient mixtures to form SOA<sub>AQ</sub>.

## 1 Introduction

Aqueous multiphase chemistry has the potential to alter the climate-relevant  
50 properties and behavior of atmospheric aerosols. It is well established that a major  
pathway for secondary organic aerosol (SOA) formation is via the partitioning of semi-  
volatile products of gas-phase photochemical reactions into preexisting organic  
particulate matter (Seinfeld and Pankow, 2003). Semi-volatile partitioning theory is  
widely used to model SOA (Odum et al., 1996; Seinfeld and Pankow, 2003; Donahue et  
55 al., 2006). However differences between organic aerosol mass/properties predicted via



this formation mechanism and measured in the atmosphere suggest that other processes (e.g., aqueous chemistry) may also contribute (Foley et al., 2010; Hallquist et al., 2009).

Recent studies have highlighted the importance of water-soluble organic gases (WSOGs), liquid water, and condensed-phase reactions to SOA formation and properties  
60 (Ervens et al., 2011; Monge et al., 2012; Carlton and Turpin, 2013). Biogenic and anthropogenic gas-phase precursors are oxidized to form WSOGs such as glyoxal, methylglyoxal, glycolaldehyde, and acetone (Spaulding et al., 2003). These WSOGs are too volatile to form SOA through absorptive partitioning, but they can undergo aqueous reactions in clouds, fogs, and wet aerosols to form low-volatility products and “aqueous”  
65 SOA (SOA<sub>AQ</sub>) (Blando and Turpin, 2000; Ervens et al., 2004; Kroll et al., 2005; Liggio et al., 2005; Lim et al., 2005; Heald et al., 2006; Loeffler et al., 2006; Sorooshian et al., 2006; Volkamer et al., 2006; Volkamer et al., 2007; Ervens et al., 2008; De Haan et al., 2009a; El Haddad et al., 2009; Ervens et al., 2011; Rossignol et al., 2014). Inclusion of aqueous chemistry of clouds, fogs, and wet aerosols in models and experiments helps to  
70 explain SOA discrepancies, particularly high atmospheric O/C ratios, enrichment of organic aerosol aloft, and formation of oxalate, sulfur- and nitrogen-containing organics and high molecular weight compounds (Kawamura and Ikushima, 1993; Kawamura et al., 1996; Crahan et al., 2004; Kalberer et al., 2004; Herrmann et al., 2005; Altieri et al., 2006; Carlton et al., 2006; Heald et al., 2006; Volkamer et al., 2007; Nozière and  
75 Cordova, 2008; De Haan et al., 2009b; El Haddad et al., 2009; Galloway et al., 2009; Shapiro et al., 2009; Volkamer et al., 2009; Lim et al., 2010; Lin et al., 2010; Nozière et al., 2010; Perri et al., 2010; Sareen et al., 2010; Schwier et al., 2010; Sorooshian et al., 2010; Sun et al., 2010; Ervens et al., 2011; Lee et al., 2011; Tan et al., 2012; Ervens et



al., 2013; He et al., 2013; Gaston et al., 2014; Ortiz-Montalvo et al., 2014). Although  
80 uncertainties are large, modeling studies show that SOA<sub>AQ</sub> is comparable in magnitude to  
“traditional” SOA (Carlton et al., 2008; Fu et al., 2008; Fu et al., 2009; Gong et al., 2011;  
Myriokefalitakis et al., 2011; Liu et al., 2012; Lin et al., 2014). However, SOA<sub>AQ</sub>  
precursors and their chemical evolution remain poorly understood.

Much of what we know about aqueous chemistry leading to SOA<sub>AQ</sub> formation is  
85 derived from laboratory studies with single precursors hypothesized to be important;  
however, the most important precursors for SOA<sub>AQ</sub> formation in the ambient  
environment may remain unidentified. A small number of studies conducted with  
ambient mixtures have provided insights into the pathways of SOA<sub>AQ</sub> formation. For  
example, photochemical oxidation of aerosol filter samples and cloud water from  
90 Whistler, British Columbia suggest that water-soluble organic compounds of intermediate  
volatility (e.g. *cis*-pinonic acid) can be important precursors for SOA<sub>AQ</sub> (Lee et al., 2012).  
Pyruvic acid oxidation experiments in Mt. Tai, China cloud water suggested a slowing of  
pyruvic acid oxidation presumably due to competition for OH radicals with the complex  
dissolved cloud water organics (Boris et al., 2014). However, further work is needed to  
95 identify precursors important for ambient SOA<sub>AQ</sub> formation in atmospheric waters.

This work reports, for the first time, results of aqueous OH radical oxidation  
experiments conducted in ambient mixtures of water-soluble gases. Ambient mixtures  
were collected in the Southeast US during the Southern Oxidant and Aerosol Study  
(SOAS) in the summer of 2013; experiments were used to identify water-soluble gases  
100 that may serve as precursors of atmospheric aqueous SOA. This region has experienced  
an overall cooling trend in surface temperature over the second half of the twentieth



century, compared to the warming trend observed elsewhere in the US (Robinson et al., 2002; Goldstein et al., 2009; Portmann et al., 2009). Biogenic sources dominate emissions in this region with varying degrees of impact from anthropogenic sources.

105 Measurements by Nguyen et al. (2014) and model results by Carlton and Turpin (2013) indicate the significance of (anthropogenic) aerosol liquid water (ALW) in this region and support a role for ALW in SOA<sub>AQ</sub> formation. In the Southeast US, photochemistry and abundant liquid water coexist, making it an ideal location to study SOA<sub>AQ</sub> formation through gas-phase followed by aqueous-phase chemistry. The objective of this work is to  
110 identify WSOGs important to SOA<sub>AQ</sub> formation. Since OH oxidation experiments were conducted in dilute solution, we will also identify products expected through cloud/fog processing of ambient WSOG mixtures. Products may differ in aerosols, where solute concentrations are higher, and radical-radical chemistry and acid-catalyzed reactions (e.g. epoxide ring-opening reactions yielding tetrols and organosulfates from IEPOX) are  
115 important. We expect that aqueous chemistry in clouds, fogs and wet aerosols is a sink for reactants identified herein, and that this work will motivate laboratory studies and chemical modeling of newly identified aerosol/cloud precursors.

## 2 Methods

120 Samples collected in mist chambers during the SOAS field study were used to conduct controlled aqueous OH radical oxidation experiments.

### 2.1 Mist chamber field sampling at SOAS (in Brent, AL)



Water-soluble gases were scrubbed from filtered ambient air at the Centerville

125 ground site in Brent, AL during SOAS. Samples were collected from June 1 – July 14, 2013. Four mist chambers (Anderson et al., 2008a; Anderson et al., 2008b; Dibb et al., 1994; Hennigan et al., 2009) were operated in an air-conditioned trailer (indoor temperature, 25°C) at 25 L min<sup>-1</sup> in parallel for 4 hours, typically 2-3 times each day between 7 AM and 7 PM CDT. Particles were removed by passing the ambient air 130 through a pre-baked quartz fiber filter (QFF) (Pall, 47mm) prior to introduction into the mist chamber. The QFF will remove particles. In the early stages of sampling, on the clean filter, adsorption of gases on the filter will reduce the concentrations of gases sampled by the mist chamber until these gases reach gas phase – adsorbed phase equilibrium. Using glyoxal as a WSOG-surrogate and the work of (Mader and Pankow, 135 2001) we predict that the measured WSOG in the mist chamber will be depleted for less than 2% of our sampling time (after <0.1 m<sup>3</sup>). Thus, we expect water-soluble gases to penetrate through the QFF very efficiently for collection in the mist chamber water.

The mist chambers were operated with 25 mL of 17.5 ± 0.5 MΩ ultra-pure water; 140 additional water was added during the run to replace water lost by evaporation. Samples from all four mist chambers were composited daily and frozen in 35 – 40 ml (experiment-sized) aliquots. Total organic carbon (TOC) concentrations ranged from 45 – 180 µM-C (Supplementary Table S1). Prior to and at the end of a sampling day, each mist chamber was cleaned using a 5-minute DI water wash step. Additionally, after the rinse step, a 2-minute dynamic blank run was conducted with activated carbon adsorbent upstream of 145 the mist chamber to remove organic gases in the flow stream.



Based on daily forecast predictions, certain days were selected for intensive sampling (Supplementary Table S1). Intensive sampling during SOAS was conducted on days when high levels of isoprene, sulfate, and  $\text{NO}_x$  were predicted by the National Center for Atmospheric Research (NCAR) using the Flexible Particle dispersion model 150 (FLEXPART) (Stohl et al., 2005) and the Model for Ozone and Related Chemical Tracers (MOZART) (Emmons et al., 2010). In general, mist chamber samples on intensive sampling days had higher organic content (TOC = 92-179  $\mu\text{M-C}$ ), and hence we focused our experiments on those days (Table 1).

Two pieces of evidence suggest that gas-aqueous partitioning of the water-soluble 155 organic gases is close to Henry's Law equilibrium in our samples. In previous testing conducted in a different East Coast location that is a recipient of long-range transport (central New Jersey) we found that WSOG concentrations in the mist chamber leveled off after 1-3 hours of ambient sampling, suggesting that the collected WSOG mixture approaches Henry's law equilibrium over these collection times. This is consistent with 160 the one measurement we have of breakthrough at SOAS, where we ran two mist chambers in series and found TOC concentrations within +/- 11% of each other. Clearly quantification of individual species will require further work. However, these measurements suggest that the mist chamber samples contain a representative mixture of water-soluble gases.

165

## 2.2 Aqueous OH radical oxidation in a cuvette chamber

Ambient SOAS field samples were exposed to OH radicals in a custom built photochemical temperature-controlled (25°C) quartz cuvette reaction chamber. Ten



screw-capped quartz cuvettes (Spectrocell Inc., Oreland, PA) containing 3 mL of sample  
170 were placed equidistant around a 254 nm mercury lamp (Heraeus Noblelight, Inc. Duluth,  
GA) housed in a quartz sheath (Ace Glass Inc., Vineland, NJ). A solar spectrum lamp  
was not used because the objective was to produce OH radicals by H<sub>2</sub>O<sub>2</sub> photolysis,  
rather than to mimic tropospheric photolysis. The chamber was protected from ambient  
light by covering in aluminum foil. OH radicals ( $1.25 \times 10^{-2}$   $\mu\text{M} [\text{OH}] \text{ s}^{-1}$ ) were generated  
175 *in situ* by photolysis of 125  $\mu\text{M}$  H<sub>2</sub>O<sub>2</sub>, added to each cuvette prior to inserting the lamp.  
Cuvettes were removed at  $t = 10, 20, 30, 40, 60, 80, 100, 120, 150$  min and any  
remaining H<sub>2</sub>O<sub>2</sub> was destroyed by addition of 36  $\mu\text{L}$  of 1% catalase (Sigma; 40,200  
units/mg). A duplicate cuvette was removed at  $t=40$  min to calculate method precision.  
The following control experiments were performed: 1) sample + H<sub>2</sub>O<sub>2</sub>, 2) sample + UV,  
180 3) H<sub>2</sub>O<sub>2</sub> + UV, and 4) field water blank + OH. Replicate experiments were performed on  
selected samples. Ambient conditions for sample collection are given in Table 1 for  
samples used in experiments.

### 2.3 Analytical methods

185 Samples and field water blanks from all collection days were characterized by  
total organic carbon analysis (TOC; Shimadzu 5000A) and electrospray ionization mass  
spectrometry (ESI-MS; HP – Agilent 1100). Ion Chromatography (IC; Dionex ICS 3000)  
was used to analyze organic anions and track the formation of products and  
intermediates. Samples at each reaction time were analyzed by ESI-MS in positive and  
190 negative ion modes to identify precursors and products. Selected samples were also  
analyzed by ultra-high resolution electrospray ionization Fourier-transform ion cyclotron



resonance mass spectrometry (ESI-FT-ICR-MS) and tandem MS (MS-MS) on a Thermo-Finnigan LTQ-XL at Woods Hole Oceanographic Institute, MA to determine elemental composition and extract structural information on precursors. Analytical details and  
195 quality control measures have been described previously (Perri et al., 2009).

Briefly, the ESI quadrupole mass spectrometer was operated in positive and negative ion modes over a mass range of 50-1000 amu. In the negative ion mode, the mobile phase consisted of 1:1 methanol/0.05% formic acid in water; and in the positive ion mode, 0.05% formic acid in water. The fragmentor and capillary voltages for the ESI-  
200 MS were set at 40 V and 3000 V (nitrogen drying gas; 10 L min<sup>-1</sup>; 350 °C), respectively. Nitrobenzoic acid in the negative ion mode and caffeine in the positive ion mode were used as mass calibrants. Standard mixtures were analyzed with each experimental sequence: acetic acid, pyruvic acid, nitric acid, succinic acid, tartaric acid, ammonium sulfate, and oxalic acid in the negative ion mode and glyoxal, methylglyoxal, and  
205 glycolaldehyde in the positive ion mode.

ESI ionization efficiency varies with sample mix and over time. However, the mass spectra of the mist chamber samples were similar across experimental days and the variability in the glyoxal standard ESI signal was <6% across analysis days, suggesting that ion abundance trends will reflect concentration trends. Six injections were averaged  
210 for each sample and data retained for each ion abundance greater than zero within 95% confidence intervals. Ions were considered to be above detection limits if greater than the average plus three standard deviations of the water blank.

Organic acids were measured by IC (IonPac AS11-HC column; 30 °C, AG11-HC guard column) with conductivity detection (35 °C), using a milli-q water eluent and KOH



215 gradient method. For oxalate, the method precision is 22%, calculated as a pooled coefficient of variation (CV) from pairs of cuvettes removed at t=40 min. The analytical precision for oxalate is 19% (pooled CV) based on replicate analysis of 30% of samples. Analytical accuracy for oxalate is 7%. The limit of detection (LOD) for oxalate by this protocol has been previously determined to be 0.1  $\mu$ M (Perri et al., 2009).

220 Samples from June 15 and June 30, 2013 were analyzed using ultra-high resolution FT-ICR-MS in the positive ion mode using 1:1 methanol/water as the mobile phase at 4  $\mu$ L min<sup>-1</sup>, capillary temperature of 260 °C and spray voltage 3.8-4.2 kV. Weekly analysis of standards (caffeine, peptide-MRFA, ultramark, SDS, and sodium taurocholate) verified the mass accuracy < 2 ppm. Note, mass accuracy tends to decrease 225 with decreasing *m/z*, so the accuracy of masses smaller than our smallest standard (195 amu) are likely to be lower. Previously pyruvic acid and peroxyhemiacetal standards analyzed with the same protocol were within 2 - 10 ppm. Error for masses determined by difference between parent and fragment ions is larger. Five precursor masses were isolated (isolation width: *m/z* = 2) and fragmented by collision-induced dissociation 230 (CID) (normalized collision energy: 26-33%) with helium in the ion trap (IT) and infrared multi photon dissociation (IRMPD) with a CO<sub>2</sub> laser. Midas Molecular Formula Calculator (v1.1) was then used on the mass of each detected peak to determine elemental composition (within  $\pm$ 1 ppm) and calculate double bond equivalence (DBE). No restrictions were placed on the number of carbon, hydrogen, oxygen, nitrogen, sodium 235 and sulfur included in the molecular formula calculations.

Compounds are detected in the ESI-MS by forming cluster ions with hydrogen, sodium, or ammonium in the positive ion mode; compounds are sometimes hydrated with



water or methanol. In the negative ion mode, ions are deprotonated. The presence of an even or odd mass provides insight into the elemental formula of the compound. For 240 instance, an even mass is an indication of a nitrogen-containing compound due to the addition of hydrogen to the odd numbered bonding of nitrogen (e.g.  $N + 3H + 1H_{\text{ionization}} = 18$  amu).

### 3 Results & Discussion

245 OH oxidation experiments at concentrations relevant to cloud/fog water were conducted on samples collected June 11, 12, 15, 16, 20, 21, 29, and 30 of 2013, days on which total organic carbon (TOC) was highest, ranging from 92-179  $\mu\text{M-C}$  in samples.

#### 3.1 Precursors in SOAS samples

250 The concentration dynamics in experiments conducted with the 8 daily composites were similar. Positive ions at  $m/z$  125, 129, 143, 173, and 187 exhibited reactant-like trends (Figure 1; June 30 sample + OH), showing decreasing signal intensity with longer exposure to OH. All the peaks disappeared after 40 minutes of oxidation. In 255 control experiments the abundance of these ions did not change over time, as illustrated in Figure 1 (sample + UV and sample +  $\text{H}_2\text{O}_2$ ) for the positive ion at  $m/z$  187 in samples collected on June 15 and 30. Hence, reaction with UV or  $\text{H}_2\text{O}_2$  alone does not explain the decreasing signals in the presence of OH radical. Experiments conducted on all sample days showed the same reactants decreasing with exposure to OH, indicating that the



260 water-soluble organics captured from the ambient daytime air in the mist chambers varied  
little across the study.

As discussed above, all precursor ions appear in the positive ion mode of the ESI-MS, consistent with the presence of carbonyl compounds and polyols. They are odd ions, suggesting they are likely not nitrogen-containing species. Elemental formulae assigned  
265 to precursor ions (using Midas) and MS-MS fragmentation data for the corresponding ions from June 15 and 30 samples are shown in Table 2. Both sampling days showed similar fragmentation spectra, consistent with the presence of the same compounds on both days, despite potential differences in the air mass from these days. No fragmentation occurred for positive ions at  $m/z$  143, 129 and 125. Proposed structures for the positive  
270 ions at  $m/z$  187 and 173 are shown in Figures 2 and 3. Possible structures for the other ions are shown in Figure 5. As seen in the proposed structures, the parent compounds contain multiple -OH groups, suggesting that they are polyols or aldehydes in the gas-phase and are hydrated with water or methanol in our ESI-MS. The O:C ratio for the reactant masses range from 0.1 - 0.8. In the following sections, we discuss individual  
275 reactants observed in the ESI-MS.

**$m/z$  187:** This is the ion with the largest  $m/z$  we observe with the ESI-MS in the positive ion mode that follows a precursor-like trend (Figures 1 and 2). Using the exact mass of 187.0942 from the FT-ICR MS, the Midas molecular formula calculator gives a formula of  $C_7H_{16}O_4Na$ , corresponding to the composition  $C_7H_{16}O_4$  for the neutral  
280 compound. (The discussion below is focused on the molecular formulas, rather than the detected ions, i.e.  $Na^+$  or  $H^+$ .) The daughter ion peak seen during fragmentation of the positive ion at  $m/z$  187 corresponds to  $m/z$  155.0680,  $CH_3OH$  loss, corresponding to the



molecular formula,  $C_6H_{12}O_3$ . We propose that this compound is present in the gas-phase as the  $C_6H_{12}O_3$  aldehyde and in water as the  $C_6H_{14}O_4$  tetrol shown in Figure 2.  $C_6H_{12}O_3$  is  
285 consistent with an oxidation product of *E*-2-hexenal and *Z*-3-hexenal, both being unsaturated aldehydes that have frequently been detected during field studies and are emitted to the atmosphere from vegetation due to leaf wounding (O'Connor et al., 2006). The oxidation mechanism of these two green leaf volatiles to form  $C_6H_{12}O_3$  is shown in Figure 3.

290 ***m/z* 173:** On most sampling days this reactant mass has the highest ion abundance in the ESI-MS operated in positive ion mode (Supplementary Figure S1). Similar to the other peaks, it reacts away within the first 40 minutes of exposure to OH in the cuvette chamber (Figure 1). The Midas-suggested molecular formula for this parent ion mass (*m/z* 173.0782) and its two fragment ions at *m/z* 141.0523 and 129.0524 are  $C_6H_{14}O_4$ ,  
295  $C_5H_{10}O_3$ , and  $C_4H_{10}O_3$ , respectively (a reactive parent ion with the formula  $C_4H_{10}O_3$  was also observed, and is discussed below).

A compound with a molecular formula of  $C_5H_{10}O_3$  (the same mass as a fragment ion discussed above) was observed in the gas-phase in the same location (Centerville field site) by high-resolution time-of-flight chemical ionization mass spectrometry  
300 (HRTToF-CIMS) (Lee et al., 2014), coupled to a filter inlet for gases and aerosols (FIGAERO) (Lopez-Hilfiker et al., 2015; Lopez-Hilfiker et al., 2014). This could be the same compound that we measure as *m/z* 173.0782, as explained below. Note that the HRTToF-CIMS employed iodide ionization, which forms organic-iodide adducts, resulting in a virtually fragmentation free ionization. Gas phase measurements from the HRTToF-  
305 CIMS were made in real time through a 3/4" PTFE inlet operated at 16 standard  $L\ min^{-1}$ .



Isoprene hydroxy hydroperoxide (ISOPOOH) and isoprene epoxide (IEPOX) are both detected at this mass, but HRTToF-CIMS is more sensitive to ISOPOOH. ISOPOOH is an OH oxidation product of isoprene, which is further oxidized by OH under low-NO conditions to form isomeric isoprene epoxydiols (IEPOX) (Paulot et al., 2009). Both 310 IEPOX and ISOPOOH are prevalent at the SOAS ground site due to the abundance of isoprene emissions in this forested region, but it is likely that  $m/z$  173 is not indicative of these two compounds in our samples. As discussed below in detail, based on ESI-MS measurements with an IEPOX standard, it can be confirmed that IEPOX was not detected in the mist chamber samples. The O-O peroxide bond in ISOPOOH is the weakest bond 315 in the molecule, and hence when undergoing MS-MS, should be the first to fragment. There is no evidence of this bond breaking in the fragmentation spectra for  $m/z$  173, leading to the conclusion that the detected compound is not ISOPOOH. IEPOX and ISOPOOH were present in the ambient air at the field site. We expect that they were lost during sampling or storage.

320 A likely structure for positive mode  $m/z$  173 is shown in Figure 4. In this case the compound is proposed to be a  $C_5H_{10}O_3$  aldehyde in the gas phase and a  $C_5H_{12}O_4$  tetrol in water. In the FT-ICR-MS it is seen hydrated with methanol. The parent ion at  $m/z$  173 loses methanol to form  $C_5H_{10}O_3$  ( $m/z$  141.0523), and it also loses  $C_2H_4O$  to form  $C_4H_{10}O_3$  ( $m/z$  129.0524).  $C_5H_{10}O_3$  is consistent with the oxidation product of (*E*)-2-methyl-2-butenal, another green leaf volatile (Figure 3c) (Jiménez et al., 2009; Lanza et al., 2008). 325 It has also been reported as an isoprene oxidation product (Yu et al., 1995).

**Positive ions at  $m/z$  143, 129, and 125:** No fragments were observed for these reactants with MS-MS. The Midas-predicted molecular formulae for the ions at  $m/z$



143.0676, 129.0520, and 125.096 are  $C_5H_{12}O_3$ ,  $C_4H_{10}O_3$ , and  $C_8H_{12}O$ , respectively.

330  $C_5H_{12}O_3$  and  $C_4H_{10}O_3$  were also seen in the gas phase at the Centerville field site by HRTToF-CIMS. Possible structures for these compounds based on their elemental formula and double bond equivalents are shown in Figure 5. Interestingly, the reactant detected at  $m/z$  129 has the same mass as a fragment of the parent ion at  $m/z$  173 discussed earlier (and the structure of the  $C_4H_{10}O_3$  fragment shown in Figure 4 is another possible structure 335 for  $m/z$  129).

Figure S2 shows time series of ion abundance in the aqueous mist chamber samples (8-12 hr integrated samples) and gas-phase signals of compounds with corresponding molecular formulas as measured by HRTToF-CIMS (Lee et al., 2014; Lopez-Hilfiker et al., 2014). There are not strong correlations, but there are similarities in 340 trends. Note that ionization of compounds in the ESI-MS and CIMS varies with compound class and with the composition of the mixture (matrix); instrument sensitivity varies daily. In some cases, more than one isomer (with the same mass) may contribute to the observed signal and isomers with the same mass may contribute differently to the CIMS and ESI-MS signal strength (e.g.,  $m/z$  173). Also, the ESI-MS measurements were 345 made after collection in water, whereas CIMS measurements were made in the gas phase. Thus, there are limitations to quantitative comparisons between these measurements in the absence of authentic standards. However, measurement of the same masses and the similarities in trends suggest that we may be measuring the same or similar species.

We expected IEPOX and glyoxal to be present in the samples since they were 350 detected in the gas-phase during the SOAS campaign (Nguyen et al., 2015) (glyoxal by Keutsch group) and have relatively high Henry's Law constants, but we did not detect



either of these compounds in our samples using our ESI-MS. Average gas-phase concentrations of IEPOX and glyoxal were measured to be ~0.09 ppb and 0.1 ppb, respectively (Nguyen et al., 2015) (glyoxal by Keutsch group), which based on their 355 Henry's Law constants ( $H_{L,IEPOX}=2.7 \times 10^6 \text{ M atm}^{-1}$ ,  $H_{L,GLYOXAL}=3.6 \times 10^5 \text{ M atm}^{-1}$ ) correspond to ~250  $\mu\text{M}$  IEPOX and 36  $\mu\text{M}$  glyoxal in the aqueous phase. When the ambient samples were spiked with 3000  $\mu\text{M}$ , 300  $\mu\text{M}$ , and 30  $\mu\text{M}$  standards of either compound, they were readily detected, indicating that they can be ionized in our sample matrix. (Authentic *trans*- $\beta$ -IEPOX, which is the predominant isomer of IEPOX, was 360 synthesized for this purpose (Zhang et al. (2012).) It is quite likely that these compounds are too unstable to persist through collection and storage in our aqueous samples. In fact, they may have oxidized during collection, since water-soluble oxidants would have also been scrubbed by the mist chambers).

365 **3.2 Product formation during aqueous oxidation experiments**

Figure 6 shows significant formation of oxalate and pyruvate in OH radical experiments conducted with all samples but not during the control experiments (Sample + UV; Sample +  $\text{H}_2\text{O}_2$ ). Pyruvate peaks around 60-80 min, which is earlier than the oxalate 370 peak at 100-120 min (Figure 6). Acetate + glycolate (which co-elute in the IC) also forms in at least some samples and reacts away in the presence of OH (Supplementary Figure S3). Sulfate and nitrate concentrations remained constant throughout the experiment as measured by the IC. While there may be many sources of oxalate, aqueous OH radical oxidation of pyruvate in the aqueous phase is known to form oxalate at dilute (cloud-



375 relevant) concentrations (Carlton et al., 2006). Aqueous acetate oxidation is also a source of oxalate (Tan et al., 2012). The concentration dynamics are consistent with a role for these compounds in the formation of oxalate in the ambient mixtures although the mechanisms by which pyruvate and acetate formed are not well constrained in these experiments. These observations suggest that oxalate, pyruvate, and acetate can form in  
380 ambient mixtures of water-soluble gases in the Southeast US in the presence of clouds/fogs and oxidants. Pyruvate and oxalate have been observed primarily in the particle phase in the atmosphere (Saxena and Hildemann, 1996; Limbeck et al., 2001; Yao et al., 2002; Kawamura et al., 2003). Moreover, modeling studies of oxalate, the most abundant dicarboxylic acid in the atmosphere, suggest that aqueous chemistry is a  
385 large contributor of oxalate formation globally, making it a good tracer for SOA<sub>AQ</sub> formed in clouds and fogs (Myriokefalitakis et al., 2011). Above versus below cloud measurements also support this (Sorooshian et al., 2010). Thus, the experiments suggest that aqueous oxidation of ambient (Southeastern US) water-soluble mixtures at cloud/fog relevant concentrations has the potential to form material that remains in the particle-  
390 phase species after droplet evaporation, i.e. SOA<sub>AQ</sub>. However, the atmospheric prevalence of *particle-phase* oxalate can only be explained by the formation of salts and complexes, since oxalic acid is volatile and the volatility of oxalate salts is orders of magnitude lower than that of oxalic acid (Ortiz-Montalvo et al., 2014; Paciga et al., 2014). The aerosol at the SOAS ground site was acidic (campaign average pH~0.94)  
395 (Guo et al., 2015) and as a consequence oxalic acid may remain largely in the gas phase in this environment, but may eventually react on more basic surfaces, e.g., coarse particles. Note that we expect the products of aqueous chemistry in wet aerosols to be



different from those in clouds and fogs because of the extremely high (molar) solute concentrations in wet aerosols (Surratt et al., 2007; Noziere et al., 2008; Galloway et al., 400 Lim et al., 2010; Sareen et al., 2010; Nguyen et al., 2012).

### 3.3 Atmospheric implications

We have tentatively characterized several water-soluble OH-reactive species collected at an isoprene-rich photochemically-active location in the southeastern U.S. In 405 several cases compounds with the same elemental composition were measured in the gas phase by HRToF-CIMS. The tentative structures for the proposed reactants are consistent with formation from green leaf volatiles and isoprene oxidation. Aqueous OH oxidation under dilute conditions (TOC approx. 100  $\mu$ M) relevant to fogs and clouds produced oxalate and pyruvate suggesting that cloud/fog processing of these compounds (and 410 subsequent neutralization or complexation) is a potential source of SOA. The reactants characterized in this work are precursors for aqueous chemistry and are potentially important SOA<sub>AQ</sub> precursors in all atmospheric waters, i.e. clouds, fogs, and wet aerosols. The aqueous chemistry of these precursors is poorly understood and warrants further study.

415

### 4 Conclusions

We observed formation of pyruvate, oxalate, and acetate/glycolate during OH oxidation experiments conducted with ambient mixtures of WSOG from the southeastern US. The formation of these highly oxygenated organic acids indicates a potential for 420 SOA<sub>AQ</sub> formation (e.g., upon neutralization with NH<sub>3</sub>, metal complexation or



heterogeneous reaction on course dust/salt particles). Given the acidity of SOAS fine particles, we think it is unlikely that oxalate will be found in substantial quantities in the fine aerosol at the SOAS ground site.

We tentatively characterized several water-soluble reactive precursors of aqueous 425 chemistry and SOA<sub>AQ</sub> formation in wet aerosols, clouds and fogs at this location. High resolution mass spectrometric analyses suggest precursors had O:C ranging from 0.125-0.80 and several of them could plausibly be tied to isoprene oxidation. No distinct difference was seen in the aqueous oxidation of ambient samples collected across days during the SOAS field campaign. Further work involving organic synthesis, aqueous OH 430 oxidation of authentic standards, and mass spectral analyses with pre-separation are likely to yield further insights into the aqueous chemistry of these compounds in the future.

## 5 Acknowledgements

This research was funded by the EPA STAR grant 835412. The views expressed in this 435 manuscript are those of the authors and do not necessarily reflect the views or policies of the U.S. Environmental Protection Agency. The authors acknowledge Melissa Soule and funding sources of the WHOI FT-MS User's Facility (NSF OCE-0619608 and the Gordon and Betty Moore Foundation). We also thank Jeffrey Kirland, Ronald Lauck, and Nancy Sazo for their invaluable assistance in the laboratory and field, and Louisa 440 Emmons for the air quality forecasting during SOAS.

Supporting Information Available. Included are Table S1 and Figures S1-S3. The material is available free of charge via the Internet at <http://pubs.acs.org>.



445 **References**

Altieri, K. E., Carlton, A. G., Lim, H.-J., Turpin, B. J., and Seitzinger, S. P.: Evidence for Oligomer Formation in Clouds: Reactions of Isoprene Oxidation Products, Environmental Science & Technology, 40, 4956-4960, 10.1021/es052170n, 2006.

Anderson, C., Dibb, J. E., Griffin, R. J., and Bergin, M. H.: Simultaneous measurements of particulate and gas-phase water-soluble organic carbon concentrations at remote and urban-influenced locations, Geophysical Research Letters, 35, L13706, 10.1029/2008GL033966, 2008a.

Anderson, C. H., Dibb, J. E., Griffin, R. J., Hagler, G. S. W., and Bergin, M. H.: Atmospheric water-soluble organic carbon measurements at Summit, Greenland, Atmospheric Environment, 42, 5612-5621, <http://dx.doi.org/10.1016/j.atmosenv.2008.03.006>, 2008b.

Blando, J. D., and Turpin, B. J.: Secondary organic aerosol formation in cloud and fog droplets: a literature evaluation of plausibility, Atmospheric Environment, 34, 1623-1632, 2000.

Boris, A. J., Desyaterik, Y., and Collett, J. L.: How do components of real cloud water affect aqueous pyruvate oxidation?, Atmos Res, 143, 95-106, DOI 10.1016/j.atmosres.2014.02.004, 2014.

Carlton, A. G., Turpin, B. J., Lim, H. J., Altieri, K. E., and Seitzinger, S.: Link between isoprene and secondary organic aerosol (SOA): Pyruvic acid oxidation yields low volatility organic acids in clouds, Geophysical Research Letters, 33, Artn L06822 Doi 10.1029/2005gl025374, 2006.



Carlton, A. G., Turpin, B. J., Altieri, K. E., Seitzinger, S. P., Mathur, R., Roselle, S. J., and Weber, R. J.: CMAQ Model Performance Enhanced When In-Cloud Secondary Organic Aerosol is Included: Comparisons of Organic Carbon Predictions with  
470 Measurements, *Environmental Science & Technology*, 42, 8798-8802, 2008.

Carlton, A. G., and Turpin, B. J.: Particle partitioning potential of organic compounds is highest in the Eastern US and driven by anthropogenic water, *Atmos. Chem. Phys.*, 13, 10203-10214, 10.5194/acp-13-10203-2013, 2013.

Crahan, K. K., Hegg, D., Covert, D. S., and Jonsson, H.: An exploration of aqueous oxalic acid production in the coastal marine atmosphere, *Atmospheric Environment*, 38, 3757-3764, <http://dx.doi.org/10.1016/j.atmosenv.2004.04.009>, 2004.

De Haan, D. O., Corrigan, A. L., Smith, K. W., Stroik, D. R., Turley, J. J., Lee, F. E., Tolbert, M. A., Jimenez, J. L., Cordova, K. E., and Ferrell, G. R.: Secondary Organic  
480 Aerosol-Forming Reactions of Glyoxal with Amino Acids, *Environmental Science & Technology*, 43, 2818-2824, 2009a.

De Haan, D. O., Tolbert, M. A., and Jimenez, J. L.: Atmospheric condensed-phase reactions of glyoxal with methylamine, *Geophysical Research Letters*, 36, doi:10.1029/2009GL037441, 2009b.

485 Dibb, J. E., Talbot, R. W., and Bergin, M. H.: Soluble acidic species in air and snow at Summit, Greenland, *Geophysical Research Letters*, 21, 1627-1630, 10.1029/94GL01031, 1994.



Donahue, N. M., Robinson, A. L., Stanier, C. O., and Pandis, S. N.: Coupled Partitioning, Dilution, and Chemical Aging of Semivolatile Organics, Environmental Science & Technology, 40, 2635-2643, 10.1021/es052297c, 2006.

El Haddad, I., Yao, L., Nieto-Gligorovski, L., Michaud, V., Temime-Roussel, B., Quivet, E., Marchand, N., Sellegrí, K., and Monod, A.: In-cloud processes of methacrolein under simulated conditions - Part 2: Formation of secondary organic aerosol, Atmos. Chem. Phys., 9, 5107-5117, 10.5194/acp-9-5107-2009, 2009.

Ervens, B., Feingold, G., Frost, G. J., and Kreidenweis, S. M.: A modeling study of aqueous production of dicarboxylic acids: 1. Chemical pathways and speciated organic mass production, Journal of Geophysical Research: Atmospheres, 109, n/a-n/a, 10.1029/2003JD004387, 2004.

Ervens, B., Carlton, A. G., Turpin, B. J., Altieri, K. E., Kreidenweis, S. M., and Feingold, G.: Secondary organic aerosol yields from cloud-processing of isoprene oxidation products, Geophysical Research Letters, 35, n/a-n/a, 10.1029/2007GL031828, 2008.

Ervens, B., Turpin, B. J., and Weber, R. J.: Secondary organic aerosol formation in cloud droplets and aqueous particles (aqSOA): a review of laboratory, field and model studies, Atmos. Chem. Phys., 11, 11069-11102, 10.5194/acp-11-11069-2011, 2011.

Ervens, B., Wang, Y., Eagar, J., Leaitch, W. R., Macdonald, A. M., Valsaraj, K. T., and Herckes, P.: Dissolved organic carbon (DOC) and select aldehydes in cloud and fog water: the role of the aqueous phase in impacting trace gas budgets, Atmos. Chem. Phys., 13, 5117-5135, 10.5194/acp-13-5117-2013, 2013.



510 Foley, K. M., Roselle, S. J., Appel, K. W., Bhave, P. V., Pleim, J. E., Otte, T. L.,  
Mathur, R., Sarwar, G., Young, J. O., Gilliam, R. C., Nolte, C. G., Kelly, J. T., Gilliland,  
A. B., and Bash, J. O.: Incremental testing of the Community Multiscale Air Quality  
(CMAQ) modeling system version 4.7, *Geosci. Model Dev.*, 3, 205-226, 10.5194/gmd-3-  
205-2010, 2010.

515 Fu, T.-M., Jacob, D. J., Wittrock, F., Burrows, J. P., Vrekoussis, M., and Henze,  
D. K.: Global budgets of atmospheric glyoxal and methylglyoxal, and implications for  
formation of secondary organic aerosols, *Journal of Geophysical Research: Atmospheres*,  
113, n/a-n/a, 10.1029/2007JD009505, 2008.

Fu, T.-M., Jacob, D. J., and Heald, C. L.: Aqueous-phase reactive uptake of  
520 dicarbonyls as a source of organic aerosol over eastern North America, *Atmospheric  
Environment*, 43, 1814-1822, <http://dx.doi.org/10.1016/j.atmosenv.2008.12.029>,  
2009.

Galloway, M. M., Chhabra, P. S., Chan, A. W. H., Surratt, J. D., Flagan, R. C.,  
Seinfeld, J. H., and Keutsch, F. N.: Glyoxal uptake on ammonium sulphate seed aerosol:  
525 reaction products and reversibility of uptake under dark and irradiated conditions, *Atmos.  
Chem. Phys.*, 9, 3331-3345, 10.5194/acp-9-3331-2009, 2009.

Gaston, C. J., Thornton, J. A., and Ng, N. L.: Reactive uptake of N<sub>2</sub>O<sub>5</sub> to  
internally mixed inorganic and organic particles: the role of organic carbon oxidation  
state and inferred organic phase separations, *Atmos. Chem. Phys.*, 14, 5693-5707,  
530 10.5194/acp-14-5693-2014, 2014.

Goldstein, A. H., Koven, C. D., Heald, C. L., and Fung, I. Y.: Biogenic carbon  
and anthropogenic pollutants combine to form a cooling haze over the southeastern



United States, Proceedings of the National Academy of Sciences, 106, 8835-8840,  
10.1073/pnas.0904128106, 2009.

535 Gong, W., Stroud, C., and Zhang, L.: Cloud Processing of Gases and Aerosols in  
Air Quality Modeling, *Atmosphere*, 2, 567-616, 2011.

Guo, H., Xu, L., Bougiatioti, A., Cerully, K. M., Capps, S. L., Hite Jr, J. R.,  
Carlton, A. G., Lee, S. H., Bergin, M. H., Ng, N. L., Nenes, A., and Weber, R. J.: Fine-  
particle water and pH in the southeastern United States, *Atmos. Chem. Phys.*, 15, 5211-

540 5228, 10.5194/acp-15-5211-2015, 2015.

Hallquist, M., Wenger, J. C., Baltensperger, U., Rudich, Y., Simpson, D., Claeys,  
M., Dommen, J., Donahue, N. M., George, C., Goldstein, A. H., Hamilton, J. F.,  
Herrmann, H., Hoffmann, T., Iinuma, Y., Jang, M., Jenkin, M. E., Jimenez, J. L.,  
Kiendler-Scharr, A., Maenhaut, W., McFiggans, G., Mentel, T. F., Monod, A., Prévôt, A.

545 S. H., Seinfeld, J. H., Surratt, J. D., Szmigielski, R., and Wildt, J.: The formation,  
properties and impact of secondary organic aerosol: current and emerging issues, *Atmos.*  
*Chem. Phys.*, 9, 5155-5236, 10.5194/acp-9-5155-2009, 2009.

He, C., Liu, J., Carlton, A. G., Fan, S., Horowitz, L. W., Levy II, H., and Tao, S.:  
Evaluation of factors controlling global secondary organic aerosol production from cloud  
550 processes, *Atmos. Chem. Phys.*, 13, 1913-1926, 10.5194/acp-13-1913-2013, 2013.

Heald, C. L., Jacob, D. J., Turquety, S., Hudman, R. C., Weber, R. J., Sullivan, A.  
P., Peltier, R. E., Atlas, E. L., de Gouw, J. A., Warneke, C., Holloway, J. S., Neuman, J.  
A., Flocke, F. M., and Seinfeld, J. H.: Concentrations and sources of organic carbon  
aerosols in the free troposphere over North America, *Journal of Geophysical Research:*

555 *Atmospheres*, 111, n/a-n/a, 10.1029/2006JD007705, 2006.



Hennigan, C. J., Bergin, M. H., Russell, A. G., Nenes, A., and Weber, R. J.:

Gas/particle partitioning of water-soluble organic aerosol in Atlanta, *Atmos. Chem. Phys.*, 9, 3613-3628, 10.5194/acp-9-3613-2009, 2009.

Herrmann, H., Tilgner, A., Barzaghi, P., Majdik, Z., Gligorovski, S., Poulain, L.,

560 and Monod, A.: Towards a more detailed description of tropospheric aqueous phase  
organic chemistry: CAPRAM 3.0, *Atmospheric Environment*, 39, 4351-4363,

<http://dx.doi.org/10.1016/j.atmosenv.2005.02.016>, 2005.

Jiménez, E., Lanza, B., Antiñolo, M., and Albaladejo, J.: Influence of temperature  
on the chemical removal of 3-methylbutanal, trans-2-methyl-2-butenal, and 3-methyl-2-  
565 butenal by OH radicals in the troposphere, *Atmospheric Environment*, 43, 4043-4049,  
<http://dx.doi.org/10.1016/j.atmosenv.2009.05.005>, 2009.

Kalberer, M., Paulsen, D., Sax, M., Steinbacher, M., Dommen, J., Prevot, A. S.  
H., Fisseha, R., Weingartner, E., Frankevich, V., Zenobi, R., and Baltensperger, U.:

Identification of Polymers as Major Components of Atmospheric Organic Aerosols,  
570 *Science*, 303, 1659-1662, 10.1126/science.1092185, 2004.

Kawamura, K., and Ikushima, K.: Seasonal changes in the distribution of  
dicarboxylic acids in the urban atmosphere, *Environmental Science & Technology*, 27,  
2227-2235, 10.1021/es00047a033, 1993.

Kawamura, K., Kasukabe, H., and Barrie, L. A.: Source and reaction pathways of  
575 dicarboxylic acids, ketoacids and dicarbonyls in arctic aerosols: One year of  
observations, *Atmospheric Environment*, 30, 1709-1722,  
[http://dx.doi.org/10.1016/1352-2310\(95\)00395-9](http://dx.doi.org/10.1016/1352-2310(95)00395-9), 1996.



Kawamura, K., Umemoto, N., Mochida, M., Bertram, T., Howell, S., and Huebert, B. J.: Water-soluble dicarboxylic acids in the tropospheric aerosols collected  
580 over east Asia and western North Pacific by ACE-Asia C-130 aircraft, *Journal of Geophysical Research: Atmospheres*, 108, 8639, 10.1029/2002JD003256, 2003.

Kroll, J. H., Ng, N. L., Murphy, S. M., Varutbangkul, V., Flagan, R. C., and Seinfeld, J. H.: Chamber studies of secondary organic aerosol growth by reactive uptake  
of simple carbonyl compounds, *J. Geophys. Res.*, 110, D23207, 2005.

585 Lanza, B., Jiménez, E., Ballesteros, B., and Albaladejo, J.: Absorption cross section determination of biogenic C5-aldehydes in the actinic region, *Chemical Physics Letters*, 454, 184-189, <http://dx.doi.org/10.1016/j.cplett.2008.02.020>, 2008.

Lee, A. K. Y., Zhao, R., Gao, S. S., and Abbatt, J. P. D.: Aqueous-Phase OH Oxidation of Glyoxal: Application of a Novel Analytical Approach Employing Aerosol  
590 Mass Spectrometry and Complementary Off-Line Techniques, *The Journal of Physical Chemistry A*, 115, 10517-10526, 10.1021/jp204099g, 2011.

Lee, A. K. Y., Hayden, K. L., Herckes, P., Leaitch, W. R., Liggio, J., Macdonald, A. M., and Abbatt, J. P. D.: Characterization of aerosol and cloud water at a mountain site during WACS 2010: secondary organic aerosol formation through oxidative cloud  
595 processing, *Atmos. Chem. Phys.*, 12, 7103-7116, 10.5194/acp-12-7103-2012, 2012.

Lee, B. H., Lopez-Hilfiker, F. D., Mohr, C., Kurtén, T., Worsnop, D. R., and Thornton, J. A.: An Iodide-Adduct High-Resolution Time-of-Flight Chemical-Ionization Mass Spectrometer: Application to Atmospheric Inorganic and Organic Compounds,  
Environmental Science & Technology, 48, 6309-6317, 10.1021/es500362a, 2014.



600 Liggio, J., Li, S. M., and McLaren, R.: Heterogeneous reactions of glyoxal on particulate matter: Identification of acetals and sulfate esters, *Environmental Science & Technology*, 39, 1532-1541, 2005.

Lim, H.-J., Carlton, A. G., and Turpin, B. J.: Isoprene Forms Secondary Organic Aerosol through Cloud Processing: Model Simulations, *Environmental Science & Technology*, 39, 4441-4446, 10.1021/es048039h, 2005.

605 Lim, Y. B., Tan, Y., Perri, M. J., Seitzinger, S. P., and Turpin, B. J.: Aqueous chemistry and its role in secondary organic aerosol (SOA) formation, *Atmos. Chem. Phys.*, 10, 10521-10539, 10.5194/acp-10-10521-2010, 2010.

Limbeck, A., Puxbaum, H., Otter, L., and Scholes, M. C.: Semivolatile behavior 610 of dicarboxylic acids and other polar organic species at a rural background site (Nylsley, RSA), *Atmospheric Environment*, 35, 1853-1862, [http://dx.doi.org/10.1016/S1352-2310\(00\)00497-0](http://dx.doi.org/10.1016/S1352-2310(00)00497-0), 2001.

Lin, G., Sillman, S., Penner, J. E., and Ito, A.: Global modeling of SOA: the use 615 of different mechanisms for aqueous-phase formation, *Atmos. Chem. Phys.*, 14, 5451-5475, 10.5194/acp-14-5451-2014, 2014.

Lin, P., Huang, X.-F., He, L.-Y., and Zhen Yu, J.: Abundance and size distribution of HULIS in ambient aerosols at a rural site in South China, *Journal of Aerosol Science*, 41, 74-87, <http://dx.doi.org/10.1016/j.jaerosci.2009.09.001>, 2010.

Liu, J., Horowitz, L. W., Fan, S., Carlton, A. G., and Levy, H.: Global in-cloud 620 production of secondary organic aerosols: Implementation of a detailed chemical mechanism in the GFDL atmospheric model AM3, *Journal of Geophysical Research: Atmospheres*, 117, n/a-n/a, 10.1029/2012JD017838, 2012.



Loeffler, K. W., Koehler, C. A., Paul, N. M., and De Haan, D. O.: Oligomer

formation in evaporating aqueous glyoxal and methyl glyoxal solutions, Environmental

625 Science & Technology, 40, 6318-6323, 2006.

Lopez-Hilfiker, F. D., Mohr, C., Ehn, M., Rubach, F., Kleist, E., Wildt, J.,

Mentel, T. F., Lutz, A., Hallquist, M., Worsnop, D., and Thornton, J. A.: A novel method  
for online analysis of gas and particle composition: description and evaluation of a Filter

Inlet for Gases and AEROSols (FIGAERO), Atmos. Meas. Tech., 7, 983-1001,

630 10.5194/amt-7-983-2014, 2014.

Lopez-Hilfiker, F. D., Mohr, C., Ehn, M., Rubach, F., Kleist, E., Wildt, J.,

Mentel, T. F., Carrasquillo, A. J., Daumit, K. E., Hunter, J. F., Kroll, J. H., Worsnop, D.  
R., and Thornton, J. A.: Phase partitioning and volatility of secondary organic aerosol  
components formed from  $\alpha$ -pinene ozonolysis and OH oxidation: the importance of

635 accretion products and other low volatility compounds, Atmos. Chem. Phys., 15, 7765-  
7776, 10.5194/acp-15-7765-2015, 2015.

Mader, B. T., and Pankow, J. F.: Gas/Solid Partitioning of Semivolatile Organic  
Compounds (SOCs) to Air Filters. 3. An Analysis of Gas Adsorption Artifacts in  
Measurements of Atmospheric SOCs and Organic Carbon (OC) When Using Teflon

640 Membrane Filters and Quartz Fiber Filters, Environmental Science & Technology, 35,  
3422-3432, 10.1021/es0015951, 2001.

Monge, M. E., Rosenørn, T., Favez, O., Müller, M., Adler, G., Abo Riziq, A.,  
Rudich, Y., Herrmann, H., George, C., and D'Anna, B.: Alternative pathway for  
atmospheric particles growth, Proceedings of the National Academy of Sciences, 109,

645 6840-6844, 10.1073/pnas.1120593109, 2012.



Myriokefalitakis, S., Tsigaridis, K., Mihalopoulos, N., Sciare, J., Nenes, A.,

Kawamura, K., Segers, A., and Kanakidou, M.: In-cloud oxalate formation in the global troposphere: a 3-D modeling study, *Atmos. Chem. Phys.*, 11, 5761-5782, 10.5194/acp-11-5761-2011, 2011.

650 Nguyen, T. B., Lee, P. B., Updyke, K. M., Bones, D. L., Laskin, J., Laskin, A.,  
and Nizkorodov, S. A.: Formation of nitrogen- and sulfur-containing light-absorbing  
compounds accelerated by evaporation of water from secondary organic aerosols, *Journal  
of Geophysical Research: Atmospheres*, 117, D01207, 10.1029/2011JD016944, 2012.

Nguyen, T. B., Crounse, J. D., Teng, A. P., St. Clair, J. M., Paulot, F., Wolfe, G.  
655 M., and Wennberg, P. O.: Rapid deposition of oxidized biogenic compounds to a  
temperate forest, *Proceedings of the National Academy of Sciences*, 112, E392-E401,  
10.1073/pnas.1418702112, 2015.

Nguyen, T. K. V., Petters, M. D., Suda, S. R., Guo, H., Weber, R. J., and Carlton,  
A. G.: Trends in particle-phase liquid water during the Southern Oxidant and Aerosol  
660 Study, *Atmos. Chem. Phys.*, 14, 10911-10930, 10.5194/acp-14-10911-2014, 2014.

Noziere, B., Dziedzic, P., and Córdova, A.: Products and kinetics of the liquid-  
phase reaction of glyoxal catalyzed by ammonium ions (NH4+), *The Journal of Physical  
Chemistry A*, 113, 231-237, 2008.

Nozière, B., and Cordova, A.: A kinetic and mechanistic study of the amino acid  
665 catalyzed aldol condensation of acetaldehyde in aqueous and salt solutions, *Journal of  
Physical Chemistry A*, 112, 2827-2837, 2008.



Nozière, B., Ekström, S., Alsberg, T., and Holmström, S.: Radical-initiated

formation of organosulfates and surfactants in atmospheric aerosols, *Geophysical*

Research Letters

37, n/a-n/a, 10.1029/2009GL041683, 2010.

670 O'Connor, M. P., Wenger, J. C., Mellouki, A., Wirtz, K., and Munoz, A.: The  
atmospheric photolysis of E-2-hexenal, Z-3-hexenal and E,E-2,4-hexadienal, *Physical*  
*Chemistry Chemical Physics*, 8, 5236-5246, 10.1039/B611344C, 2006.

Odum, J. R., Hoffmann, T., Bowman, F., Collins, D., Flagan, R. C., and Seinfeld,  
J. H.: Gas/Particle Partitioning and Secondary Organic Aerosol Yields, *Environmental*  
675 *Science & Technology*, 30, 2580-2585, 10.1021/es950943+, 1996.

Ortiz-Montalvo, D. L., Häkkinen, S. A. K., Schwier, A. N., Lim, Y. B., McNeill,  
V. F., and Turpin, B. J.: Ammonium Addition (and Aerosol pH) Has a Dramatic Impact  
on the Volatility and Yield of Glyoxal Secondary Organic Aerosol, *Environmental*  
Science & Technology, 48, 255-262, 10.1021/es4035667, 2014.

680 Paciga, A. L., Riipinen, I., and Pandis, S. N.: Effect of Ammonia on the Volatility  
of Organic Diacids, *Environmental Science & Technology*, 48, 13769-13775,  
10.1021/es5037805, 2014.

Paulot, F., Crounse, J. D., Kjaergaard, H. G., Kurten, A., St Clair, J. M., Seinfeld,  
J. H., and Wennberg, P. O.: Unexpected Epoxide Formation in the Gas-Phase

685 Photooxidation of Isoprene, *Science*, 325, 730-733, DOI 10.1126/science.1172910, 2009.

Perri, M. J., Seitzinger, S., and Turpin, B. J.: Secondary organic aerosol  
production from aqueous photooxidation of glycolaldehyde: Laboratory experiments,  
*Atmospheric Environment*, 43, 1487-1497,  
<http://dx.doi.org/10.1016/j.atmosenv.2008.11.037>, 2009.



690 Perri, M. J., Lim, Y. B., Seitzinger, S. P., and Turpin, B. J.: Organosulfates from  
glycolaldehyde in aqueous aerosols and clouds: Laboratory studies, *Atmospheric*

Environment, 44, 2658-2664, <http://dx.doi.org/10.1016/j.atmosenv.2010.03.031>,  
2010.

Portmann, R. W., Solomon, S., and Hegerl, G. C.: Spatial and seasonal patterns in  
695 climate change, temperatures, and precipitation across the United States, *Proceedings of  
the National Academy of Sciences*, 106, 7324-7329, 10.1073/pnas.0808533106, 2009.

Robinson, W. A., Reudy, R., and Hansen, J. E.: General circulation model  
simulations of recent cooling in the east-central United States, *Journal of Geophysical  
Research: Atmospheres*, 107, ACL 4-1-ACL 4-14, 10.1029/2001JD001577, 2002.

700 Rossignol, S., Aregahegn, K. Z., Tiné, L., Fine, L., Nozière, B., and George, C.:  
Glyoxal Induced Atmospheric Photosensitized Chemistry Leading to Organic Aerosol  
Growth, *Environ Sci Technol*, 48, 3218-3227, 10.1021/es405581g, 2014.

Sareen, N., Schwier, A. N., Shapiro, E. L., Mitroo, D., and McNeill, V. F.:  
Secondary organic material formed by methylglyoxal in aqueous aerosol mimics, *Atmos.*

705 *Chem. Phys.*, 10, 997-1016, 10.5194/acp-10-997-2010, 2010.

Saxena, P., and Hildemann, L.: Water-soluble organics in atmospheric particles:  
A critical review of the literature and application of thermodynamics to identify candidate  
compounds, *J Atmos Chem*, 24, 57-109, 10.1007/BF00053823, 1996.

Schwier, A. N., Sareen, N., Mitroo, D., Shapiro, E. L., and McNeill, V. F.:  
710 Glyoxal-Methylglyoxal Cross-Reactions in Secondary Organic Aerosol Formation,  
*Environmental Science & Technology*, 44, 6174-6182, 10.1021/es101225q, 2010.



Seinfeld, J. H., and Pankow, J. F.: Organic atmospheric particulate material, Annu Rev Phys Chem, 54, 121-140, Doi 10.1146/Annurev.Physchem.54.011002.103756, 2003.

Shapiro, E. L., Szprengiel, J., Sareen, N., Jen, C. N., Giordano, M. R., and  
715 McNeill, V. F.: Light-absorbing secondary organic material formed by glyoxal in aqueous aerosol mimics, Atmospheric Chemistry and Physics, 9, 2289-2300, 2009.

Sorooshian, A., Varutbangkul, V., Brechtel, F. J., Ervens, B., Feingold, G.,  
Bahreini, R., Murphy, S. M., Holloway, J. S., Atlas, E. L., Buzorius, G., Jonsson, H.,  
Flagan, R. C., and Seinfeld, J. H.: Oxalic acid in clear and cloudy atmospheres: Analysis  
720 of data from International Consortium for Atmospheric Research on Transport and  
Transformation 2004, Journal of Geophysical Research: Atmospheres, 111, n/a-n/a,  
10.1029/2005JD006880, 2006.

Sorooshian, A., Murphy, S. M., Hersey, S., Bahreini, R., Jonsson, H., Flagan, R.  
C., and Seinfeld, J. H.: Constraining the contribution of organic acids and AMS m/z 44 to  
725 the organic aerosol budget: On the importance of meteorology, aerosol hygroscopicity,  
and region, Geophysical Research Letters, 37, n/a-n/a, 10.1029/2010GL044951, 2010.

Spaulding, R. S., Schade, G. W., Goldstein, A. H., and Charles, M. J.:  
Characterization of secondary atmospheric photooxidation products: Evidence for  
730 biogenic and anthropogenic sources, Journal of Geophysical Research: Atmospheres,  
108, n/a-n/a, 10.1029/2002JD002478, 2003.

Sun, Y. L., Zhang, Q., Anastasio, C., and Sun, J.: Insights into secondary organic  
aerosol formed via aqueous-phase reactions of phenolic compounds based on high  
resolution mass spectrometry, Atmos. Chem. Phys., 10, 4809-4822, 10.5194/acp-10-  
4809-2010, 2010.



735 Surratt, J. D., Lewandowski, M., Offenberg, J. H., Jaoui, M., Kleindienst, T. E.,  
Edney, E. O., and Seinfeld, J. H.: Effect of Acidity on Secondary Organic Aerosol  
Formation from Isoprene, *Environmental Science & Technology*, 41, 5363-5369,  
10.1021/es0704176, 2007.

Tan, Y., Lim, Y. B., Altieri, K. E., Seitzinger, S. P., and Turpin, B. J.:  
740 Mechanisms leading to oligomers and SOA through aqueous photooxidation: insights  
from OH radical oxidation of acetic acid and methylglyoxal, *Atmos. Chem. Phys.*, 12,  
801-813, 10.5194/acp-12-801-2012, 2012.

Volkamer, R., Jimenez, J. L., San Martini, F., Dzepina, K., Zhang, Q., Salcedo,  
D., Molina, L. T., Worsnop, D. R., and Molina, M. J.: Secondary organic aerosol  
745 formation from anthropogenic air pollution: Rapid and higher than expected, *Geophys.  
Res. Lett.*, 33, L17811, 10.1029/2006gl026899, 2006.

Volkamer, R., Martini, F. S., Molina, L. T., Salcedo, D., Jimenez, J. L., and  
Molina, M. J.: A missing sink for gas-phase glyoxal in Mexico City: Formation of  
secondary organic aerosol, *Geophysical Research Letters*, 34, 10.1029/2007gl030752,  
750 2007.

Volkamer, R., Ziemann, P. J., and Molina, M. J.: Secondary Organic Aerosol  
Formation from Acetylene ( $C_2H_2$ ): seed effect on SOA yields due to organic  
photochemistry in the aerosol aqueous phase, *Atmos. Chem. Phys.*, 9, 1907-1928,  
10.5194/acp-9-1907-2009, 2009.

755 Yao, X., Fang, M., and Chan, C. K.: Size distributions and formation of  
dicarboxylic acids in atmospheric particles, *Atmospheric Environment*, 36, 2099-2107,  
[http://dx.doi.org/10.1016/S1352-2310\(02\)00230-3](http://dx.doi.org/10.1016/S1352-2310(02)00230-3), 2002.



Yu, J., Jeffries, H. E., and Le Lachuer, R. M.: Identifying Airborne Carbonyl

Compounds in Isoprene Atmospheric Photooxidation Products by Their PFBHA Oximes

760 Using Gas Chromatography/Ion Trap Mass Spectrometry, Environmental Science &  
Technology, 29, 1923-1932, 10.1021/es00008a009, 1995.

Zhang, Z., Lin, Y. H., Zhang, H., Surratt, J. D., Ball, L. M., and Gold, A.:

Technical Note: Synthesis of isoprene atmospheric oxidation products: isomeric  
epoxydiols and the rearrangement products cis- and trans-3-methyl-3,4-

765 dihydroxytetrahydrofuran, Atmos. Chem. Phys., 12, 8529-8535, 10.5194/acp-12-8529-  
2012, 2012.



770 **Tables & Figures**

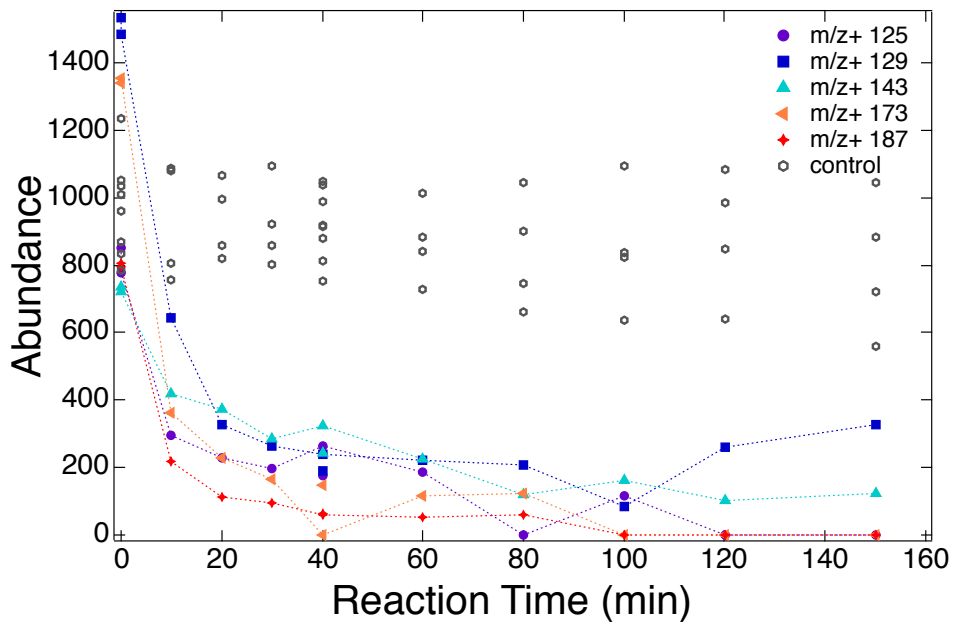
**Table 1:** Sample collection dates for which experiments were run and their sampling conditions. Temperature, relative humidity, and ozone ranges are shown both for the entire day and collection time period. Total organic carbon (TOC) accuracy and precision 775 are verified with potassium hydrogen phthalate (KHP) standards to be better than 5% (Perri et al., 2009).

Collection date	Collection time	$\mu\text{M}$ TOC	T ( $^{\circ}\text{C}$ ) all day (coll. time)	RH (%) all day (coll. time)	$\text{O}_3$ (ppbv) all day (coll. time)
11-Jun-2013	7am-7pm	139.5	22-32 (23-32)	53-99 (53-98)	9.9-38.2 (11.3-38.2)
12-Jun-2013	7am-7pm	179.7	23-33 (23-33)	48-94 (48-94)	13.1-41.8 (13.1-41.8)
15-Jun-2013	7am-7pm	117.0	17-31 (18-31)	45-94 (45-90)	11.6-53.4 (11.6-53.4)
16-Jun-2013	7am-7pm	108.2	22-32 (22-32)	53-93 (53-84)	2.6-41.7 (23.1-41.7)
20-Jun-2013	8am-5pm	131.5	20-30 (21-30)	55-98 (59-94)	4.8-52.2 (6.2-42.8)
21-Jun-2013	10am-6pm	104.4	20-30 (25-30)	50-93 (50-78)	16.6-45.2 (30.3-45.2)
29-Jun-2013	7am-7pm	92.0	21-31 (22-31)	43-100 (43-100)	16.3-53.7 (16.3-53.7)
30-Jun-2013	7am-7pm	98.7	20-30 (20-30)	38-100 (38-100)	1-53.5 (1-53.5)



780 **Table 2:** Elemental formulas assigned to precursor ions using ESI-FT-ICR MS in the positive ionization mode and Midas Molecular Formula Calculator. MS/MS fragmentation data is also shown.

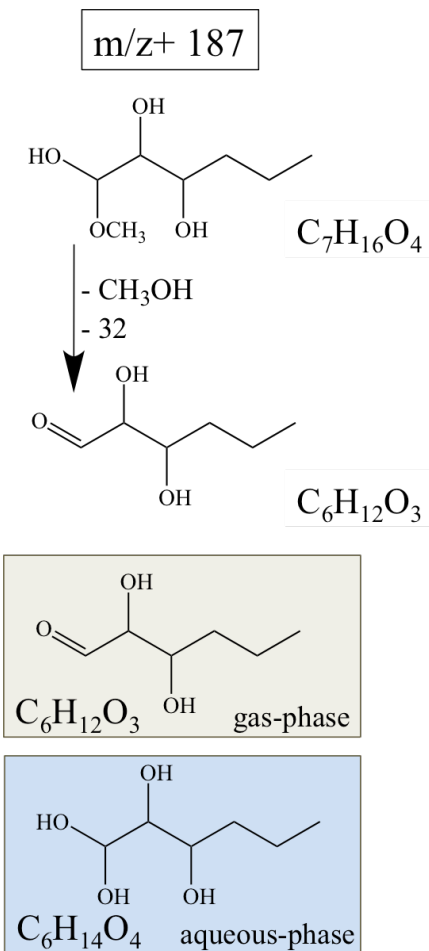
Precursor peak using ESI-MS	Positive mode <i>m/z</i> (using FT-ICR)	$[M+Na]^+$ or $[M+H]^+$	Mol. Wt.	Double bond equivalence
187	187.0942	$C_7H_{16}O_4Na$	164.1043	0
	155.0680	$C_6H_{12}O_3Na$	132.0786	1
173	173.0782	$C_6H_{14}O_4Na$	150.0887	0
	141.0523	$C_5H_{10}O_3Na$	118.0625	1
	129.0524	$C_4H_{10}O_3Na$	106.0625	0
143	143.0676	$C_5H_{12}O_3Na$	120.0781	0
129	129.0520	$C_4H_{10}O_3Na$	106.0625	0
125	125.096	$C_8H_{13}O$	124.0883	3



785

**Figure 1.** Positive ions (ESI-MS) exhibiting precursor-like trends during aqueous OH-radical oxidation experiments with the ambient mixtures collected on June 30. All days show similar trends, with all 5 reactant masses showing statistically significant decreasing trends as compared to the control experiments. Controls (sample + UV, sample +  $\text{H}_2\text{O}_2$ ) shown for  $m/z$  187; other masses show similar trends.

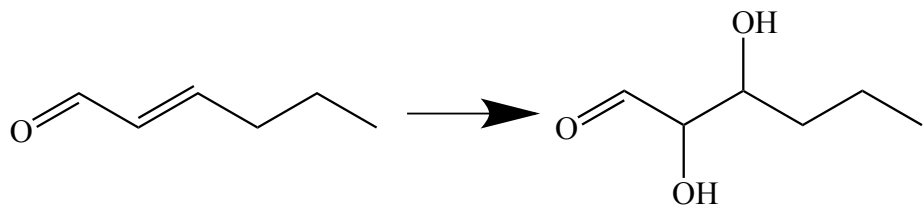
790



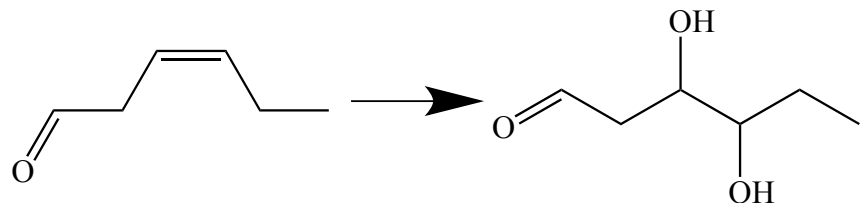
795 **Figure 2.** Proposed structure for the positive ion at  $m/z$  187. The top structure is the parent compound detected as a reactant in the ESI-MS; the following structures show the MS/MS fragments. The respective gas-phase and aqueous-phase compounds are shown in the shaded boxes at the bottom.



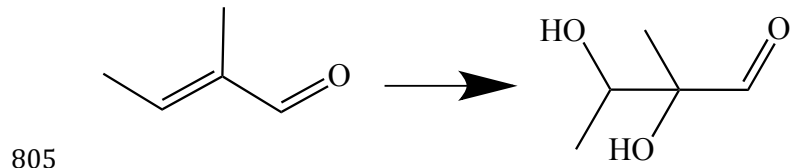
800 (a)



(b)

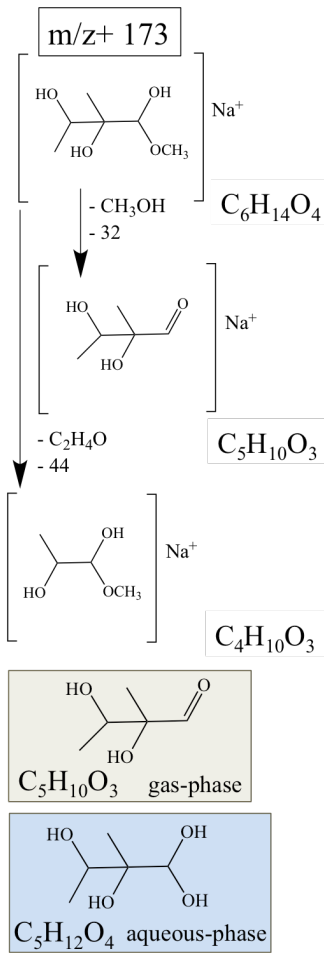


(c)



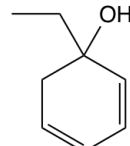
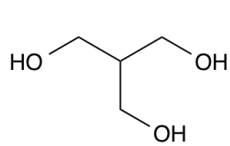
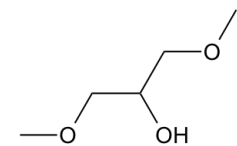
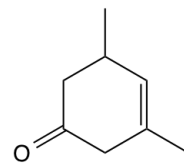
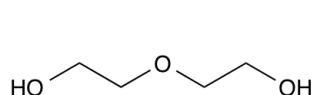
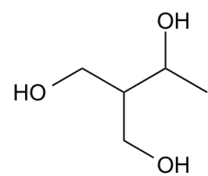
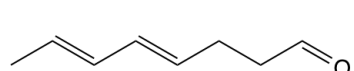
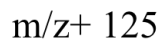
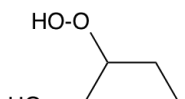
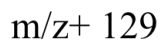
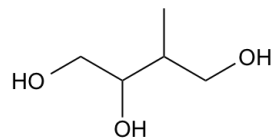
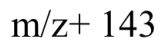
805

**Figure 3:** Gas-phase oxidation of (a) *E*-2-hexenal and (b) *Z*-3-hexenal and (c) *(E)*-2-methyl-2-butenal.



810

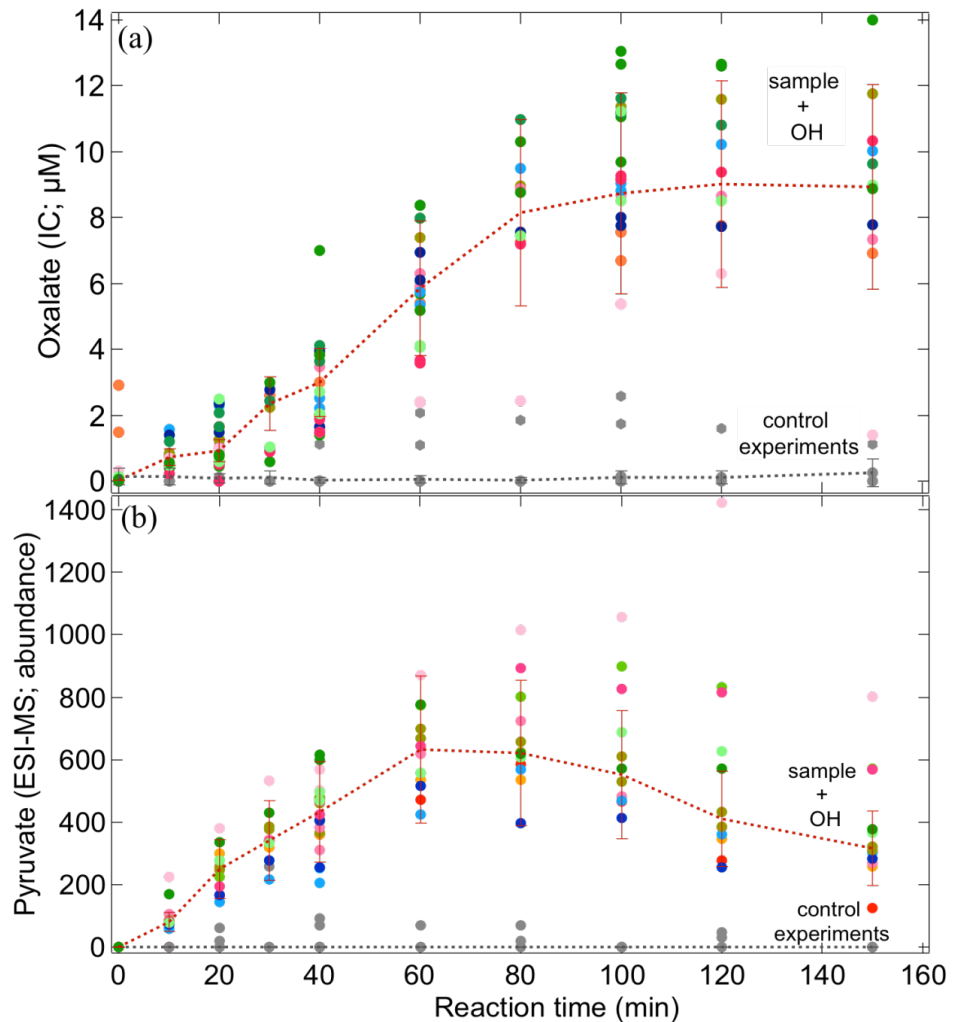
**Figure 4.** Proposed structure for the positive ion at  $m/z$  173. The top structures in each panel are the parent compound detected as a reactant in the ESI-MS; the following structures show the MS/MS fragments. The respective gas-phase and aqueous-phase compounds are shown in the shaded boxes at the bottom.



815

**Figure 5:** Possible structures for the positive ions at  $m/z$  143,  $m/z$  129, and  $m/z$  125.

These structures are based on MIDAS suggested elemental formulae for these masses and double bond equivalence (DBE). No fragmentation was observed for these reactant masses.



820

**Figure 6.** (a) Oxalate (by IC) for all OH radical oxidation experiments conducted with ambient samples (Table 1). (b) Abundance of the negative ion at  $m/z$  87 (pyruvate) as observed in the ESI-MS when the ambient SOAS samples are exposed to OH. Error bars represent the pooled coefficient of variation calculated across experimental days. Note that oxalate formed in all samples in the presence, but not the absence, of OH. Gray points represent control experiments (June 11 sample + UV, June 11 sample +  $\text{H}_2\text{O}_2$ , June 30 field water blank + OH).

825